Available online at www.sciencedirect.com

ScienceDirect

Energy Procedia 4 (2011) 1403–1410

Energy Procedia

www.elsevier.com/locate/procedia

GHGT-10

Feasibility study of CO_2 capture by anti-sublimation

Marc-Oliver Schach[a*], Bernardo Oyarzún[b], Henning Schramm[c], Rüdiger Schneider[c], Jens-Uwe Repke[a]

[a]Institute of Thermal, Environmental and Natural Products Process Engineering, TU Bergakademie Freiberg, Leipziger Straße 28, 09596 Freiberg, Germany
[b]Process & Energy Department, Delft University of Technology, Delft, The Netherlands
[c]Siemens AG Energy Sector, Fossil Power Generation, Industriepark Höchst, 65926 Frankfurt am Main

Abstract

Processes for carbon capture and storage have the drawback of high energy demand. In this work the application of CO_2 capture by anti-sublimation is analyzed. The process was simulated using Aspen Plus. Process description is accomplished by phase equilibria models which are able to reproduce the vapor-liquid and vapor-solid equilibria. Different process configurations are proposed. Total electric energy demand was defined as the evaluation criteria and the most suitable configuration was selected within technical limits. Further performance enhancement was achieved by improving the compression cooling cycles. An economic evaluation was performed for the low temperature process and the results were compared to a chemical absorption process with monoethanolamine. CO_2 capture by anti-sublimation showed a better performance concerning the energy demand but with a reduced economic benefit due to higher equipment cost.

Keywords: CO_2 capture, anti-sublimation, simulation, process design

1. Introduction

Carbon capture and storage techniques have been extensively developed and analyzed in the last years as an alternative for reducing CO_2 emissions to the atmosphere. Many processes for CO_2 capture have been proposed which can be generally classified in precombustion, postcombustion and oxyfuel capture. In this work a low temperature CO_2 postcombustion capture process at atmospheric pressure is proposed for conditions typically found in a conventional coal-fired power plant. 90% of the CO_2 emissions should be separated from the flue gas. The process was simulated and designed using Aspen Plus®. For a comprehensive process evaluation an economic analysis was performed.

* Corresponding author. Tel.: +49 3731 39-3344; fax: +49 3731 39-3652
E-mail address: Marc-Oliver.Schach@tun.tu-freiberg.de

doi:10.1016/j.egypro.2011.02.005

Separation of CO_2 from flue gases at atmospheric pressure and low temperatures requires cooling down the flue gas to the sublimation temperature determined by the partial pressure of CO_2 in the flue gas. The flue gas coming out of a typical coal-fired power plant after the sulfur removal consists of nitrogen N_2, carbon dioxide CO_2, oxygen O_2 and water H_2O. For the aim of this work other minor constituents like sulfur oxides SOx, nitrogen oxides NOx and dust are not considered. The flue gas composition used in this work is typical for coal-fired power plants and shown in Table 1.

The capture process consists of different separation steps. First the flue gas is cooled down by direct contact cooling with water. This is a common step when treating the flue gas in a chemical absorption desorption process. The composition after this stage is also shown in Table 1. In the adjacent steps water is completely removed, first as liquid and below the triple point as ice. The dry flue gas is further cooled down until CO_2 precipitates. The phase behavior during the separation steps was calculated using Aspen Plus®. The phase equilibria modeling is described in the next section.

Table 1: Typical flue gas composition after sulphur removal and after water cooling

		After SO_2 removal	*After water cooling*
Mass flow		779.5 kg/s	747.6 kg/s
Temperature		324,5 K (51,3°C)	312.8 K (39,6°C)
% mole	CO_2	14.0	15.0
	H_2O	13	7
	N_2	70	75
	O_2	3	3

2. Phase equilibria modeling

CO_2 separation from flue gases at low temperatures involves precipitation processes based on phase equilibria behavior of the involved species. Phase equilibria and process calculations were carried out employing the software Aspen Plus®. The phase equilibra condition expressed as equalitiy of fugacities in a mixture is specified by

$$f_i^I = f_i^{II} \tag{1}$$

$$\varphi_i^I x_i^I P = \varphi_i^{II} x_i^{II} P \tag{2}$$

Equation (2) is known as the φ-φ criteria for phase equilibrium. Equation of state (EoS) models define a relation between P-V-T variables. In this work the Peng-Robinson EoS [1] was selected. The binary interaction parameters k_{ij} are determined by adjusting the model to phase equilibria experimental data and were taken from Knapp [2].Vapor-solid equilibria can be represented in Aspen Plus® only as chemical reactions equivalent processes. In this description phase transition is understood as a "reaction" of the component from the solid to the vapor phase. Equation (3) represents the vapor-solid phase equilibria of CO_2 as a reaction equivalent process.

$$CO_{2(solid)} \leftrightarrow CO_{2(vapor)} \tag{3}$$

In order to describe the equilibria state, a sublimation equivalent chemical equilibria relation is introduced, equation (4).

$$-\frac{\Delta G_{sub}^0}{RT} = \ln K_{sub} = \frac{\ln a^{vapor}}{a^{solid}} \tag{4}$$

K_{sub} is defined as the sublimation equilibrium constant, ΔG_{sub} is standard Gibbs energy of sublimation and a the activity of the component in the vapor or solid phase. Activity is defined as the deviation of the chemical potential of a component from a defined standard state or equivalent as the ratio of the fugacity of a component in a mixture f_i to the fugacitiy of a component in its standard state f_{i0}. For gases f_i is defined

by equation (2) and f_{i0} is equal to the standard state pressure P_0 which is usually set to 1 bar. In a pure solid phase a good approximation is to define the activity with the value of 1. This is true because in a pure solid phase, the partial molar fugacity f_i is equal to the fugacitiy of the pure component f^0_i and since the properties of solids are slightly influenced by pressure, f^0_i is close to the sublimation pressure of the solid $P_{i,sat}$. The standard state fugacity of a solid is defined by its vapor pressure $P_{i,sat}$ and therefore the ratio of partial molar fugacity to standard state fugacity for a pure solid phase approaches 1. Equation (5) summarizes the equilibria relation for a sublimation process.

$$-\frac{\Delta G^0_{sub}}{RT} = lnK_{sub} = \ln \prod \frac{\varphi_i y_i P}{P_0} \tag{5}$$

The standard sublimation Gibbs energy ΔG^0_{sub} at constant temperature is alternatively defined by equation (6). H^0_{sub} is the standard sublimation enthalpy and S^0_{sub} the standard sublimation entropy.

$$\Delta G^0_{sub} = \Delta H^0_{sub} - T\Delta S^0_{sub} \tag{6}$$

The dependency of the sublimation equilibrium constant K_{sub} with temperatures is specified by a Clausius-Clapeyron type relation.

$$\frac{dlnK}{dT} = \frac{\Delta H^0_{sub}}{RT^2} \tag{7}$$

The values of the sublimation parameters H^0_{sub} and S^0_{sub} are adjusted to experimental sublimation data [2] employing equations (4) and (6).

Phase equilibria calculations involving vapor-solid equilibria were carried out in Aspen Plus® with the calculation block for phase and chemical equilibria RGibbs. This block is the only one which enables vapor-solid equilibria calculations, employing a reaction-like model as described above. The principle processes involved in the CO_2 separation from flue gas at low temperature are heat transfer from the flue gas and phase separation. Flue gas cooling induces the formation of a condensed phase. Cooling and phase separation are carried out in heat exchangers which achieve a determined temperature decrease. This type of heat exchanger can be represented with RGibbs blocks. These blocks account only for the interchanged heat and determine the outlet conditions from phase equilibria calculations. Heat and mass transfer effects are not considered. Cooling/separation processes take place over an extended surface by which temperature is continuously decreased. If only one RGibbs block is used for a cooling/separation stage, the whole process would be simulated at only one temperature and component properties like sublimation enthalpy would not be correctly reproduced with the model. The implemented model should consider this process behavior. In order to get close to a continuous temperature decrease, each cooling/separation stage was discretized arithmetically in many steps. After 10 steps the addition of one step more reduced the relative deviation on a factor less than 2*10-2 and was not considered as a significant improvement in the simulation. Thus each cooling/separation stage was reproduced using 10 temperature steps.

3. Process Design

During the separation process at atmospheric pressure and low temperatures the flue gas is cooled down to the sublimation temperature determined by the partial pressure of CO_2 in the flue gas. Further cooling decreases the amount of CO_2 in the gaseous phase until a specific temperature determined by the CO_2 separation degree is reached. Cooling down the flue gas from its initial temperature H2O condenses before CO_2 starts to precipitate. H_2O is first separated as water and then as ice when the partial pressure of H_2O lays under the pressure of the triple point of water. Figure 1 shows the partial pressures of CO_2 and H_2O in the flue gas as a function of temperature. The arrows indicate the direction that partial pressures follow as the temperature decreases in the separation process. CO_2 and H_2O pure component phase diagrams are included in order to identify the phases involved in the process. Correlations for these phase diagrams were taken from Span [3] and Wagner [4]. The lowest temperature reached in the process determines the amount

of CO_2 separated from the flue gas. Figure 2 indicates the separation degree of CO_2 as a function of temperature at a total pressure of 0.1 MPa for the flue gas. The required condition of 90% separation is reached at 155 K.

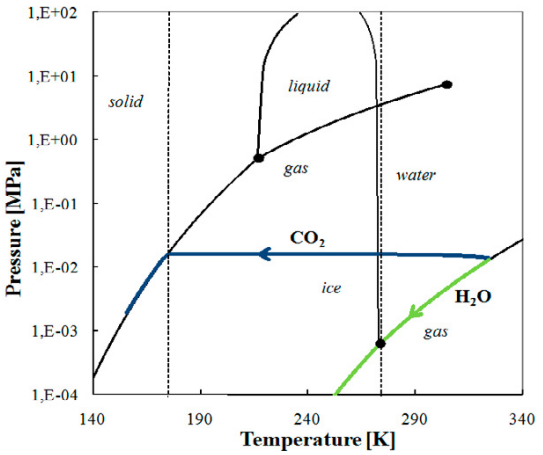

Figure 1: CO_2 and H_2O partial pressure across the process. Heavy solid lines, partial pressure of CO_2 and H_2O. Fine solid lines, phase diagram of CO_2 and H_2O.

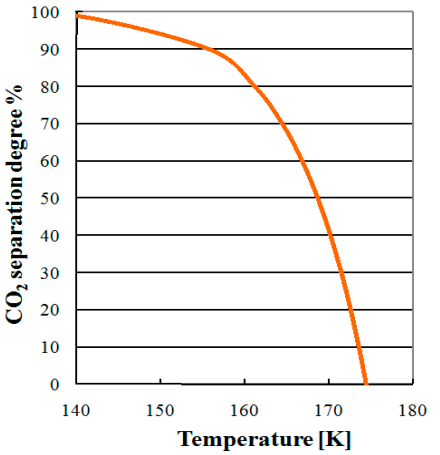

Figure 2: CO_2 separation degree as a function of the temperature.

A block diagram of the CO_2 separation process at low temperatures is shown in Figure 3. Each stage is designated by the component and phase that is separated from the flue gas. Flue gas enters the process at 325 K (51°C) and leaves the CO2 separation stage at 155 K. The inlet temperature is still high enough for cooling down with water at atmospheric conditions. A first step of cooling by direct contact with water is considered. The flue gas temperature is reduced to 313 K (40°C). The temperature at the outlet of the first separation stage corresponds to the temperature of the triple point of water plus one degree, 274 K. Outlet temperature of the second separation stage corresponds to the CO2 saturation temperature of the flue gas plus one degree, 175 K. The temperature was decreased in each stage to one degree over the limit temperature of phase transition in order to clearly separate different operations. Temperature of the last separation stage corresponds to the temperature for 90% CO_2 separation degree, 155 K. Formation of hydrates in the solid H2O separation stage was not considered due to the low concentration of water in this operation. For transport and storage purposes the separated CO_2 has to be compresses to 11 MPa and cooled down to 313 K (40°C). Pressure drop has to be overcome and a blower was connected to the process entry for this purpose.

Cooling and phase separation are achieved in heat exchangers that remove heat and the condensed phase from the flue gas. Depending on the condensed phase, two classes of heat exchangers can be identified, liquid removal and solid removal heat exchanger. Liquid separation is achieved by gravity and water flows continuously out of the heat exchanger. Solid separation involves the problem of solid formation and removal. In the designed process two parallel connected heat exchangers are required. While one heat

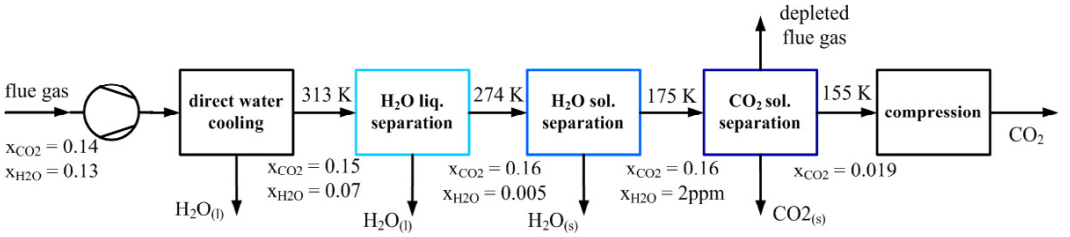

Figure 3: Block diagram of the CO_2 separation process at low temperatures

exchanger is getting loaded with the separated solid on its surface, the second is regenerated by means of a hot stream and the separated solid component is sublimated from the exchanger surface. The gaseous stream is alternated between heat exchangers and a cooling or heating medium is employed. Clodic [5] employed this arrangement for semi-continuous separation of solid CO_2 from a gaseous stream.

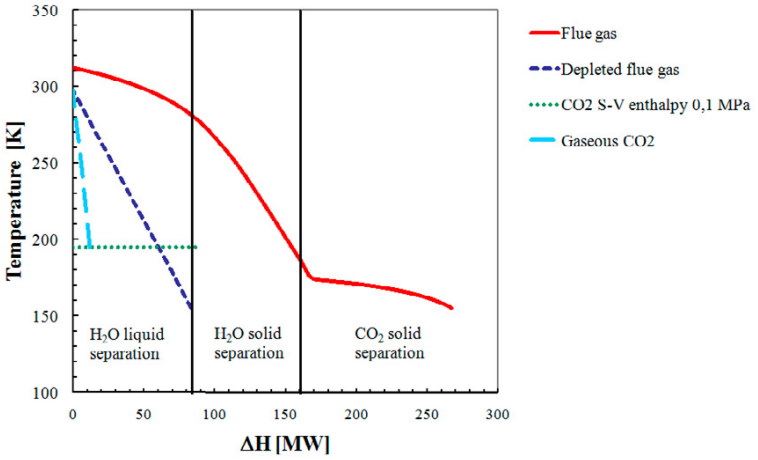

Figure 4: Temperature – enthalpy change diagram of the process

The enthalpy change of the flue gas across the separation units determines the cooling requirement for the process. Outgoing streams leave the process at low temperature and integration to the process would reduce the total external cooling requirement. Figure 4 illustrates the temperature - enthalpy change diagram of the process. The hot side (flue gas after direct cooling with water) and the cold side (cool streams for heat integration) are shown. For heat integration purposes the enthalpy change of the exhaust gas by heating it up to ambient temperature and the sublimation enthalpy of solid CO_2 can be used.

Heat integration was carried out setting a minimal temperature approach of 5 K. It can be observed that the curves of exhaust gas and gaseous CO_2 after sublimation have a similar slope as the flue gas cooling curve at the solid H_2O separation. Thus heat integration of the two gaseous streams was conducted for the solid H_2O separation step. Temperature, enthalpy and phase transition of solid CO_2 depends on the pressure of the system. Three cases can be regarded for the heat integration of the solid CO_2: sublimation of CO_2 at low pressure, sublimation of CO_2 at atmospheric pressure and fusion of CO_2 at a pressure just above the triple point. Cooling requirements after heat integration are completed by compression cooling cycles. The different alternatives are compared on the basis of total electric energy demand for the compressors in the cooling cycles. The best solution with an energy demand of 112 MW would be the sublimation of the CO_2 at low pressure. Since the required pressure is very low (0.0009 MPa) this option was discarded due to the expected problems during the technical realization. A more technical suitable approach is to remove the CO_2 from the heat exchanger as a liquid. Liquefaction takes place at pressures over the triple point (0.52 MPa). The enthalpy of fusion can be integrated to the first flue gas cooling stage. This option requires 276 MW of electric energy. The last alternative explores the integration of sublimating CO_2 at 0.1 MPa. In order to take advantage of the low temperature reached by the sublimation process, integration of solid – vapor transition is not directly integrated to the flue gas cooling but to the cooling cycle arrangement in the solid CO_2 separation stage. This option which required 232 MW of electric energy was selected as the preferred alternative for this process. Figure 5 shows the developed process diagram for the selected alternative.

Since the energy demand even with heat integration is still very high, improvements were proposed for the cooling cycles. Increasing the number of compression stages reduced the required electric energy. Three stages were chosen for each cooling cycle for the solid CO_2 separation stage.

Additionally the temperature levels at which cooling/separation of liquid H_2O and solid CO_2 takes place were increased by one level for each separation task. By applying these improvements to the cooling cycles the electric energy demand could be decreased by 34% to 153 MW which implies a specific energy demand of 0.193 kWh/kg CO_2. This value is comparable to those reported by Clodic et al. [5].

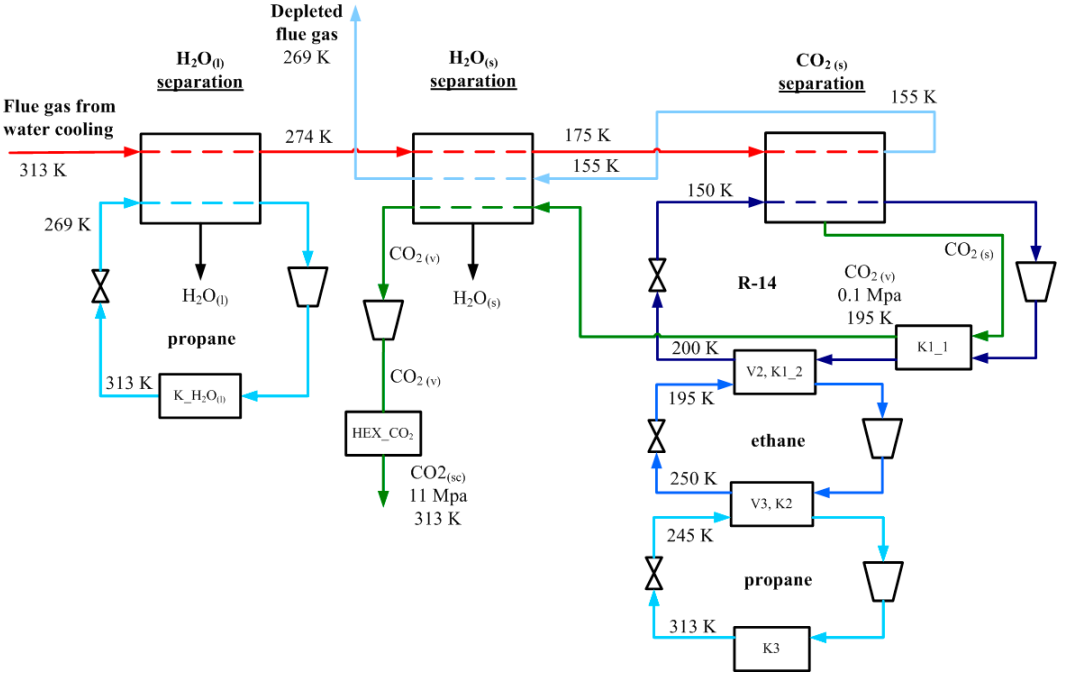

Figure 5: Process diagram of the three separation stages with heat integration

4. Layout and Economic Analysis

Basic layout and economical analysis for the low temperature CO_2 separation process designed in the previous section is carried in this chapter. Principal equipments required for the separation process are selected and sized based on the flue gas characteristics defined in Table 1. Total capital investment for the selected equipment is estimated and represent together with the calculated cost of CO_2 avoided the economic parameters for the separation alternative. Process and economic parameters are compared with values previously obtained for the reference monoethanolamine (MEA) process [6].

The principle components required for this process are compressors and heat exchangers. Compression is carried out in multi-stage compressors by which compression ratios between 2:1 – 6:1 are required. Centrifugal compressors are selected for all compressors in the process. A polytropic efficiency of 85% was assumed for the compressors.

Before selecting heat exchangers, pressure drop has to be considered. Increasing pressure drops raises proportionally the power requirement of the process and reduces the feasibility of this alternative. In order to find a good compromise between pressure drop and power demand a maximum pressure drop of 0.03 MPa is defined for the entire process which means 0.1 MPa for each separation stage (liquid water, ice and solid CO_2). Blower energy demand reaches 25 MW for this pressure drop. Three types of heat exchangers are qualitatively analyzed for this process. Shell-tube heat exchangers are commonly used in the process industry. The pressure drop is determined by heat exchanger design. Low pressure drop arrangements can be achieved but with a low heat exchanger area density. Plate-fin heat exchangers are formed by a series of plates and fins stacked in a column. Heat transfer takes place between the fluid and plates and the fluid and fins increasing the available area for heat transfer. They have a higher density of heat exchanger area than

shell-tube exchangers with moderate pressure drop. Coil-wound heat exchangers consist of tubes coiled inside a shell. Their heat exchange area density is comparable with those of plate-fin heat exchangers but with a larger pressure drop. For the analyzed process plate-fin heat exchanger were selected. The calculated required heat exchange areas are shown in Table 2. A heat transfer coefficient of 100 W/m^{2}K for gas-gas heat transfer and 50 W/m^{2}K for gas-gas heat transfer with solid formation were estimated [7, 8].

Table 2: Total heat exchange rates and required heat transfer areas for each cooling/separation stage

	Q [MW]	*A [m^2]*
Liquid H_2O separation	93.3	78,663
Solid H_2O separation	75.2	73,567
Solid CO_2 separation	98.8	233,865

Plate-fin heat exchangers are available with different geometric characteristics in terms of fin thickness, fin height and fin pitch [9, 10]. However, applying the available heat exchanger geometries the selected pressure drop could only be reached by increasing the heat exchange area over the required value. To satisfy the pressure drop conditions with the heat exchange area shown in Table 2 the geometry parameter had to be adjusted. In order to maintain a close relation with actual heat exchanger geometries the fin height to pitch ratio was kept constant at 2.7. Table 3 shows the number of parallel heat exchanger and the fin height for each separation stage. The fin height value in the second heat exchanger for H_2O liquid separation reaches a value of 118 mm. This value is far away from the real geometric range of 3.8 – 12 mm but gives an idea of the geometric conditions required for this separation stage.

Table 3: Number of parallel connected heat exchanger and fin heights for each separation stage

	Number	*Fin height [mm]*
Liquid H_2O separation HEX I	12	28.6
Liquid H_2O separation HEX II	27	118.0
Solid H_2O separation HEX I	8	7.0
Solid H_2O separation HEX II	4	17.4
Solid CO_2 separation HEX I	8	5.3
Solid CO_2 separation HEX II	6	6.4

In the stages by which solid H_2O and CO_2 are separated a base pressure drop of 0.001 MPa is considered. Deposition of solid at the exchanger surfaces increases the pressure drop until the maximum value of 0.01 MPa for the separation stage is reached. Solid deposition leads to the formation of a solid layer over the heat exchanger surface which reduces the equivalent diameter and the pressure drop increases exponentially. A maximum frost layer for solid H_2O of 2.8 mm and 2 mm for CO_2 was calculated. This means for a semi continuous operation a switching time of 44.8 hours in the H_2O solid separation stage and of 1.3 hours in the CO_2 solid separation stage.

For a comprehensive evaluation of the process an economic analysis was carried out. Capital cost and operation and maintenance cost were taken into account. The compositions of these cost were estimated according to Peters et al. [11]. All cost were converted into a constant series of payments for every year of project life which was assumed to be 25 years. The plant operates 7500 h/year and the interest rate was set to 8%. Process and economic parameters resume the principal characteristics and requirements for the proposed CO_2 capture alternative. The principle process and economic parameters related to the low temperature CO_2 separation process developed in this work are shown in Table 4. Parameter values for CO_2 separation using monoethanolamine (MEA) were taken from [6]. For parameters associated with cost data only the ratio between the two processes is shown.

On a generally perspective it can be concluded that the low temperature CO_2 separation process has a better energetic performance than the CO_2 capture with monoethanolamine but with a reduced economic benefit due to the high investments related to the equipment.

Table 4: Summary of the results for the low temperature process and the reference MEA process

	MEA	*Low temperature*
Power plant efficiency loss	12.5 %	10.7 %
Total electric power demand	209 MW	178 MW
Specific electric demand	0.391 kWh/kg CO2	0.286 kWh/kg CO2
Purchased equipment cost	1	2.58
Cost of CO_2 avoided	1	1.46

5. Conclusion

The basic design of a process for postcombustion capture of CO_2 from the flue gas of a typical coal-fired power plant was proposed in this study. Thermodynamic basics and models required for process simulation were identified and implemented in the simulation software Aspen Plus®. Total electric energy demand was used as the comparison parameter between alternatives. Selection between process alternatives was achieved not only considering a reduced electric energy demand but also practical aspects concerning technical implementation of the process. For a comprehensive evaluation a first economic analysis was performed. The final process was compared with a CO_2 capture process based on chemical absorption with monoethanolamine. The low temperature process showed a better performance concerning the energy demand but a reduced economic benefit in terms of cost of CO_2 avoided due to the large investment cost for the required equipment.

6. References

[1] Peng, D., Robinson, D.B., A new two-constant equation of state, Industrial & Engineering Chemistry Fundamentals, 15(1), 59 – 64, 1976.

[2] Knapp, H., Vapor-liquid equilibria for mixtures of low-boiling substances, Dechema Chemistry Data Series, Vol. VI, 1989.

[3] Span, R., A new equation of state for carbon dioxide covering the fluid region from the triple point temperature to 1000 K at pressures up to 800 MPa, Journal of Physical and Chemical Reference Data, 25(6), 1509 – 1596, 1996.

[4] Wagner W., Saul, A., Pruss, A., International equations for the pressure along the melting and along the sublimation curve of ordinary water substances, Journal of Physical and Chemical Reference Data, 23(3), 515 – 527, 1994.

[5] Clodic, D., El Hitti, R., Younes, M., Bill, Alain, Casier, F., CO2 capture by anti-sublimation Thermo-economic process evaluation, Paper presented at the 4th Annual Conference on Carbon Capture & Sequestration, 2005.

[6] Schach, M.-O., Schneider, R., Schramm, H., Repke, J.-U., Techno-Economic Analysis of Postcombustion Processes for the Capture of Carbon Dioxide from Power Plant Flue Gas, Ind. Eng. Chem. Res., 49, 2363 – 2370, 2010.

[7] Xia, Y., Zhong, Y., Hrnjak, P., Jacobi, A., Frost, defrost, and refrost and its impact on the air-side thermal-hydraulic performance of louvered-fin, flat-tube heat exchangers, International Journal of Refrigeration, 29(7), 1066 – 1079, 2006.

[8] Zhang, P., Hrnjak, P., Air-side performance evaluation of three types of heat exchangers in dry, wet and periodic frosting conditions, International Journal of Refrigeration, 32(5), 911 – 921, 2009.

[9] The Standards of the Brazed Aluminium Plate-fin Heat Exchanger Manufacturer's Association, 2nd ed., 2000.

[10] Aluminium Plate-Fin Heat Exchangers, product catalog, Linde AG, 2009.

[11] Peters, M.S., Timmerhaus, K.D., West, R.E., Plant Design and Economics for Chemical Engineers, 5th ed., McGraw-Hill Professional: New York, 2002.